

## Stationary self-localized states due to quadratic nonlinearity in one-dimensional systems

This article has been downloaded from IOPscience. Please scroll down to see the full text article.

1998 J. Phys.: Condens. Matter 10 2701

(<http://iopscience.iop.org/0953-8984/10/12/010>)

View [the table of contents for this issue](#), or go to the [journal homepage](#) for more

Download details:

IP Address: 171.66.16.209

The article was downloaded on 14/05/2010 at 16:21

Please note that [terms and conditions apply](#).

# Stationary self-localized states due to quadratic nonlinearity in one-dimensional systems

Anandamohan Ghosh<sup>†</sup>, B C Gupta and K Kundu

Institute of Physics, Bhubaneswar-751 005, India

Received 8 July 1997, in final form 18 November 1997

**Abstract.** We investigate the effect of a nondegenerate quadratic nonlinear dimeric impurity on the formation of stationary localized states in one-dimensional systems. We also consider the formation of stationary self-localized states in a translationally invariant fully nonlinear system where alternative sites have the same nonlinear strengths. Appropriate *ansatze* have been chosen for all of the cases which reproduce the known results for special cases. The connection of the stability of a state to its energy is presented graphically.

## 1. Introduction

The discrete nonlinear Schrödinger equation (DNLSE) which describes a number of phenomena in condensed matter physics, nonlinear optics and other fields of physics [1–6] for one-dimensional systems is generally written as

$$i \frac{dC_m}{dt} = -\chi_m f_m(|C_m|)C_m + V_{m,m+1}C_{m+1} + V_{m,m-1}C_{m-1}$$

where  $V_{m,m+1} = V_{m+1,m}^*$  and  $m = 1, 2, 3, \dots, n$ . (1)

In equation (1),  $\chi_m$  is the nonlinearity parameter associated with the  $m$ th grid point and  $V_{m,m+1}$  is the nearest-neighbour hopping matrix element. Since,  $\sum_m |C_m|^2$  is made unity by choosing appropriate initial conditions,  $|C_m|^2$  can be interpreted as the probability of finding a particle at the  $m$ th grid point. In the context of condensed matter physics, the nonlinearity term  $f_m(|C_m|)$  arises due to the coupling of the vibrations of masses at the lattice points to the motion of a quasi-particle in the high-frequency lattice vibration limit [3]. The DNLSE is known in another physical context as the discrete self-trapping (DST) equation. A number of studies of the DNLSE and DST have been reported [7–10].

As regards the application of the DNLSE specifically in condensed matter physics, we mention as an example its use in the study of exciton propagation in the Holstein molecular crystal chain [2]. In general, the exciton propagation in quasi-one-dimensional systems [11] having short-range electron–phonon interaction can be adequately modelled by the DNLSE. Other examples include its use in the study of nonlinear optical responses in superlattices formed by dielectric or magnetic slabs [12] and the mean-field theory of a periodic array of twinning planes in the high- $T_c$  superconductors [13]. We also note that the vibration in the nonlinear Klein–Gordon chain can be described by the DNLSE under certain restrictive conditions [14].

<sup>†</sup> Permanent address: Department of Physics, University of Pune, Pune-411007, India.

One important feature of the DNLS is that it can yield stationary localized (SL) states. These SL states might play a significant role in the nonlinear DNA dynamics [15] and also in the energy localization in nonlinear lattices [16]. It has been shown that the presence of a nonlinear impurity can produce SL states in one, two and three dimensions [17–24]. The formation of SL states due to the presence of a single and a degenerate dimeric nonlinear impurity in a few linear hosts has been studied in detail [20]. The same problem has also been studied starting from an appropriate Hamiltonian [23]. The fixed point of the Hamiltonian [21–24] which generates the appropriate DNLS can also produce the correct equations governing the formation of SL states. We further note that the appropriate *ansatz* for the dimer problem was obtained in our earlier analysis [20]. Furthermore, the formation of intersite peaked and dipped stationary self-localized states has been studied using the dimeric *ansatz* [24]. The formation of SL states in a perfect nonlinear chain containing one nonlinear impurity as well as a degenerate nonlinear dimeric impurity has been studied [24]. In another study the formation of SL states in a perfect nonlinear Cayley tree and in a linear Cayley tree with dimeric impurity has been considered [24].

So far, only degenerate nonlinear dimer impurities have been considered. Naturally, the question arises of what happens if the impurities in the dimer are nondegenerate. We therefore plan to study the effect of nondegeneracy in impurities on the formation of SL states. Three linear hosts are studied, namely a perfect one-dimensional chain, a Cayley tree and a linear chain with a bond defect. We also consider the formation of SL states in a fully nonlinear chain having a regular binary alloy composition. Appropriate *ansatze* have been fitted in all of the cases to obtain the results.

The organization of the paper is as follows. In section 2 we consider the effect of a nonlinear nondegenerate dimer on the formation of SL states in linear systems. Section 3 deals with the formation of SL states in a fully nonlinear system and the stability analysis of the SL states. We summarize our findings in section 4. Finally there is an appendix in which we demonstrate the transformation of the Cayley tree into an effective one-dimensional system.

## 2. Nondegenerate nonlinear dimer impurities

We consider a one-dimensional chain system consisting of a nondegenerate nonlinear dimer impurity of the kind  $\chi|C|^\sigma$  (a power-law impurity) where  $\sigma$  is arbitrary. The dimeric impurity is placed at sites 0 and 1 of the chain. The dimer is nondegenerate in the sense that the nonlinear strengths at sites 0 and 1 are different; these are denoted by  $\chi_0$  and  $\chi_1$ . Furthermore, the system has a bond defect between sites 0 and 1. Therefore, the relevant Hamiltonian for this system is

$$H = \sum_{m=-\infty}^{\infty} [C_m C_{m+1}^* + \text{HC}] + (V - 1)[C_0 C_1^* + \text{HC}] + \frac{2\chi_0}{\sigma + 2}|C_0|^{\sigma+2} + \frac{2\chi_1}{\sigma + 2}|C_1|^{\sigma+2}. \quad (2)$$

The hopping matrix element connecting sites 0 and 1 is  $V$  and the others are taken to be unity. In the absence of nonlinear impurities, the Hamiltonian with  $V = 1$  describes a perfect chain and that with  $V < 1$  corresponds to a perfect Cayley tree, as is shown in the appendix, while that with  $V > 1$  describes a one-dimensional chain with a bond defect between sites 0 and 1. Over and above, each of the systems contains a nondegenerate nonlinear dimeric impurity spanning the zeroth and first sites. Since we are interested in

the possible solutions for SL states due to the presence of dimeric impurity, we assume that

$$C_m = \phi_m e^{-iEt}. \tag{3}$$

It is well known that the impurity states in one-dimensional systems are exponentially localized. Therefore, the presence of a dimeric impurity in the system suggests that we consider the following form of  $\phi_m$ :

$$\begin{aligned} \phi_m &= [\text{sgn}(E)\eta]^{m-1} \phi_1 & m \geq 1 \\ \phi_{-|m|} &= [\text{sgn}(E)\eta]^{|m|} \phi_0 & m \leq 0. \end{aligned} \tag{4}$$

We further note that the above form for  $\phi_m$  can be derived from Green's function analysis [20]. Here  $\eta \in [0, 1]$  is given by

$$\eta = \frac{1}{2} [ |E| - \sqrt{E^2 - 4} ].$$

We further define  $\beta = \phi_1/\phi_0 \in [-1, 1]$  if  $|\phi_1| \leq |\phi_0|$ . On the other hand, for  $|\phi_0| \leq |\phi_1|$ , we can interchange the definitions of  $\beta$  without any loss of generality. Now the normalization condition,  $\sum_{m=-\infty}^{\infty} |C_m|^2 = 1$ , together with equations (3) and (4), gives

$$|\phi_0|^2 = \frac{1 - \eta^2}{1 + \beta^2}. \tag{5}$$

Using equations (3), (4) and (5) in the Hamiltonian  $H$ , we obtain the effective Hamiltonian of the reduced dynamical system:

$$\begin{aligned} H_{eff} &= 2 \text{sgn}(E)\eta + 2V\beta \frac{1 - \eta^2}{1 + \beta^2} + \frac{2}{\sigma + 2} \left( \frac{1 - \eta^2}{1 + \beta^2} \right)^{(\sigma+2)/2} \\ &\times (\chi(1 + |\beta|^{\sigma+2}) + \delta(1 - |\beta|^{\sigma+2})). \end{aligned} \tag{6}$$

Here we have defined  $\chi$  and  $\delta$  as  $\chi = (\chi_0 + \chi_1)/2$  and  $\delta = (\chi_0 - \chi_1)/2$ . For a particular system,  $\chi$  and  $\delta$  are constants while  $\eta$  and  $\beta$  are the variables.  $\eta$  and  $\beta$ , by definition, determine the energy and the probability profile of the particle in the system respectively. Therefore, these two unknown variables,  $\beta$  and  $\eta$ , need to be determined self-consistently. For this reason we treat  $\eta$  and  $\beta$  as dynamical variables of  $H_{eff}$ . SL states then can be obtained from the fixed-point solutions [21–23] of the Hamiltonian,  $H_{eff}$ , of the reduced dynamical system. The fixed-point solutions satisfy the equations  $\partial H_{eff}/\partial\beta = 0$  and  $\partial H_{eff}/\partial\eta = 0$ . In the language of the calculus of variations, we are finding extremal values of  $\beta$  and  $\eta$  using the variational principle. Since the form of the probability profile is rigorous [25], we obtain the correct values of  $\beta$  and  $\eta$ .

The equation  $\partial H_{eff}/\partial\beta = 0$  gives

$$[1 - \eta]^{\sigma/2} = \frac{V(1 - \beta^2)(1 + \beta^2)^{\sigma/2}}{\beta[(\chi + \delta) - |\beta|^\sigma(\chi - \delta)]}. \tag{7}$$

The equation  $\partial H_{eff}/\partial\eta = 0$  gives

$$\eta = \frac{\text{sgn}(E)\beta[(\chi + \delta) - |\beta|^\sigma(\chi - \delta)]}{V[(\chi + \delta) - |\beta|^{\sigma+2}(\chi - \delta)]}. \tag{8}$$

For fixed values of  $\chi$  and  $\delta$ , the number of solutions satisfying equations (7) and (8) simultaneously will give the number of possible SL states. This can be obtained for arbitrary  $\sigma$ , but we will consider  $\sigma = 0$  and  $\sigma = 2$ . The reason for selecting the  $\sigma = 0$  case is that the result is already known and hence the appropriateness of the *ansatz* can be verified.  $\sigma = 2$  is considered because it is physically more relevant.

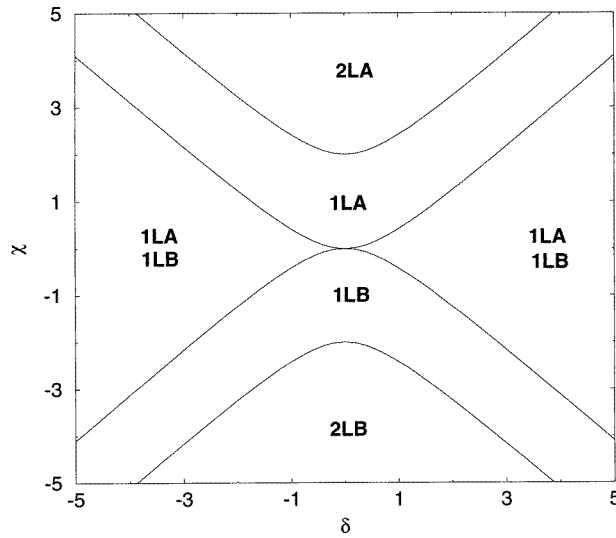


**Figure 1.** The phase diagram of SL states in the  $(\chi, \delta)$  plane for a one-dimensional system with a nondegenerate linear dimeric impurity in the middle of the system. The  $(\chi, \delta)$  plane is divided into many regions by the critical lines. The label 2LA indicates that two SL states are possible in that region and that both of them lie above the band of the linear host. Similarly, labels 1LA, 1LB and 2LB indicate regions with one SL state above the band, one SL state below the band and two SL states below the band, respectively.

### 2.1. $\sigma=0$

For  $\sigma = 0$ , the system reduces to a perfectly linear one-dimensional chain with two static impurities  $\chi_0$  and  $\chi_1$  at the sites 0 and 1 respectively. In this case, equation (7) gives directly

$$\beta_{\pm} = -\frac{\delta}{V} \pm \sqrt{\frac{\delta^2}{V^2} + 1}. \quad (9)$$

In passing, we note that, when  $\delta = 0$ , i.e. when the dimer impurity becomes linear and degenerate,  $\beta = \pm 1$  are the only permissible solutions. This is consistent with our earlier work [20]. On the other hand, for  $\delta \neq 0$  only values of  $\beta \neq \pm 1$  are permissible solutions. Substituting equation (9) in equation (8) we obtain

$$\frac{1}{\chi} = \frac{\eta}{\text{sgn}(E) \mp \eta \sqrt{\delta^2 + V^2}}. \quad (10)$$

Equation (10), along with signature of  $E$ , gives four expressions for  $1/\chi$ . From each expression we will get a critical line in the  $(\chi, \delta)$  plane. The critical lines can be obtained by putting  $\eta = 1$  in equation (10). The equations describing the critical lines are

$$\begin{aligned} \chi_c^{(1)} &= -\chi_c^{(2)} = 1 + \sqrt{\delta^2 + V^2} \\ \chi_c^{(3)} &= -\chi_c^{(4)} = 1 - \sqrt{\delta^2 + V^2}. \end{aligned} \quad (11)$$

These critical lines are shown in figure 1 for  $V = 1$ , in figure 2 for  $V = 0.5$  (which corresponds to a Cayley tree with  $K = 4$ ) and in figure 3 for  $V = \sqrt{2}$ . There are several regions in the  $(\chi, \delta)$  plane bounded by the critical lines in all of the figures. There are

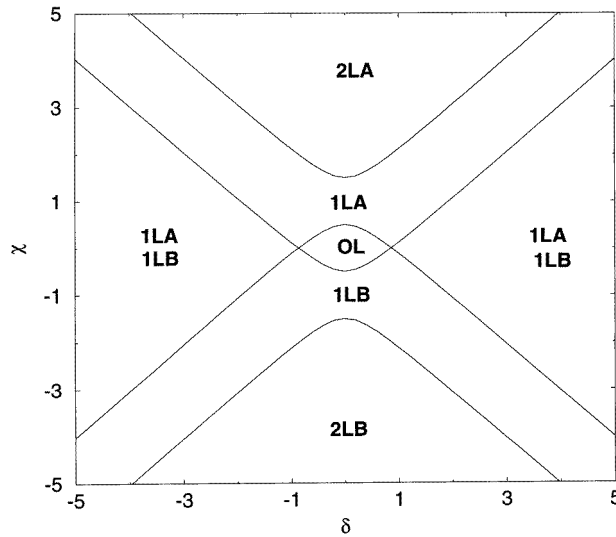


**Figure 2.** The phase diagram of SL states in the  $(\chi, \delta)$  plane for a Cayley tree with a nondegenerate linear dimeric impurity embedded in the middle of the system. The connectivity ( $K$ ) of the Cayley tree is 4. The label 0L indicates that no SL state is possible in that region. The others labels have the same meaning as in figure 1.

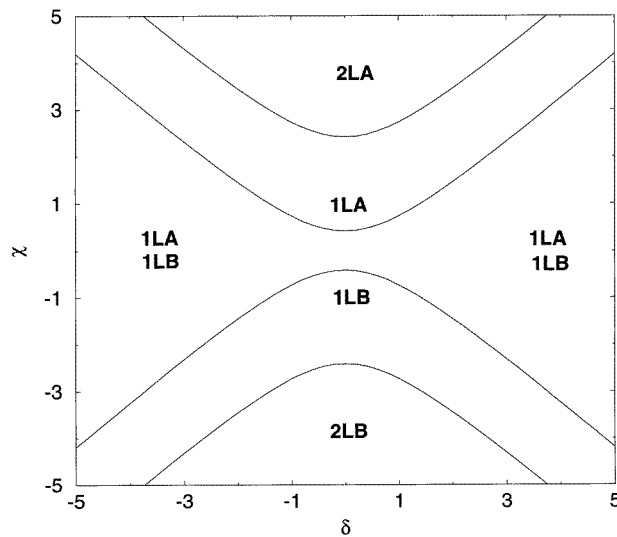


**Figure 3.** The phase diagram of SL states in the  $(\chi, \delta)$  plane for a one-dimensional system with a bond defect ( $V = \sqrt{2}$ ) between sites 0 and 1 as well as a nondegenerate linear dimeric impurity occupying sites 0 and 1. The other features are the same as for figure 1 and figure 2.

regions containing no SL state, one SL state appearing above the host band, one SL state appearing below the band, two SL states with one below and one above the band and two SL states appearing above as well as below the band. Since our results for  $V = 1$  and  $V = 0.5$  agree with known results [25], the validity of our starting *ansatz* is established.

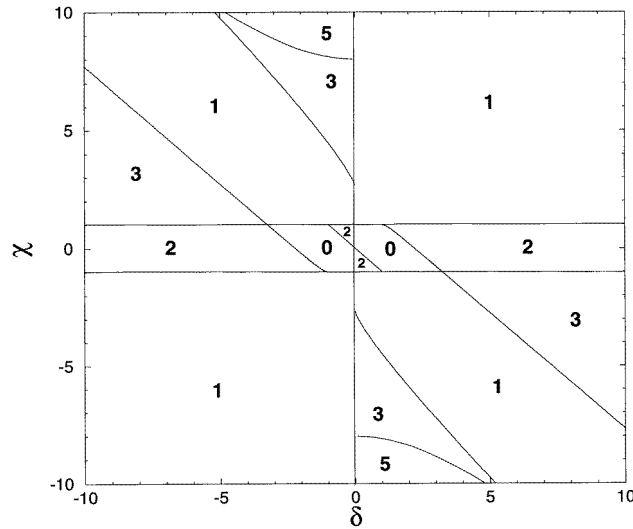


**Figure 4.** The phase diagram of SL states in the  $(\chi, \delta)$  plane for a one-dimensional system with a nondegenerate quadratic nonlinear dimeric impurity in the middle of the system. The  $(\chi, \delta)$  plane is divided into many regions by the critical lines. The number labelling a region indicates the number of SL states possible in that region.

## 2.2. $\sigma=2$

We now investigate the case in which the nonlinearity power  $\sigma = 2$ . Physically,  $\sigma = 2$  can be obtained when the masses at the lattice points are treated as Einstein oscillators. From equation (7) we again note that, for  $\delta = 0$ ,  $\beta = \pm 1$  are permissible solutions. On the other hand, for  $\delta \neq 0$ ,  $\beta = \pm 1$  are not permissible solutions. From equations (7) and (8) we obtain the relevant equation for SL states. The equation is given as

$$\frac{1}{\chi} = \frac{\beta[(1+\alpha) - (1-\alpha)\beta^2] [V^2[(1+\alpha) - (1-\alpha)\beta^4]^2 - \beta^2[(1+\alpha) - (1-\alpha)\beta^2]^2]}{V^3[1 - \beta^4][(1+\alpha) - (1-\alpha)\beta^4]^2} \quad (12)$$

where  $\alpha = \delta/\chi$ . Using equation (12) we have obtained the full phase diagram of SL states in the  $(\chi, \delta)$  plane for  $V = 1$  and this is shown in figure 4. There are various regions in the phase diagram labelled according to the numbers of SL states possible in those regions. Along the  $\delta = 0$  line, we note that, for  $\chi \geq 0$ , there are three critical values of  $\chi$ , namely, 1,  $8/3$  and 8. These critical values are in agreement with the values obtained in our earlier work [23]. In this case, the maximum number of SL states that can appear is five.

With the use of same expression, equation (12), we have also obtained the phase diagram for SL states in the  $(\chi, \delta)$  plane for a Cayley tree with connectivity  $K = 4$  ( $V = 0.5$ ). This is shown in figure 5. The maximum number of SL states possible in this case is found to be seven. The critical values of  $\chi$  along the  $\delta = 0$  line are again in agreement with our earlier result [24].

A typical phase diagram of SL states in the  $(\chi, \delta)$  plane with  $V = 2$  is also shown as figure 6. The phase diagram has regions containing one to seven SL states. Furthermore, if we compare the results for  $\delta = 0$  with those for  $\delta \neq 0$ , we note that the maximum number of SL states possible increases as nondegeneracy is introduced.

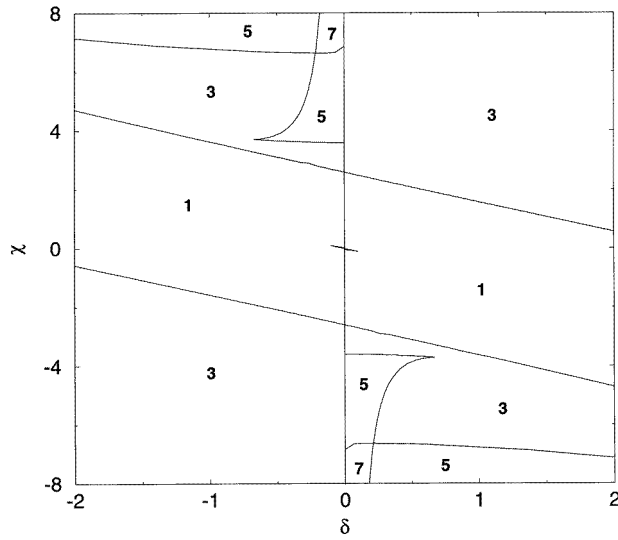


**Figure 5.** The phase diagram of SL states in the  $(\chi, \delta)$  plane for a Cayley tree with a nondegenerate quadratic nonlinear dimeric impurity embedded in the middle of the system. Here  $K = 4$ . The number labelling a region indicates the number of SL states possible in that region. There are two small unlabelled regions near the origin containing two SL states.

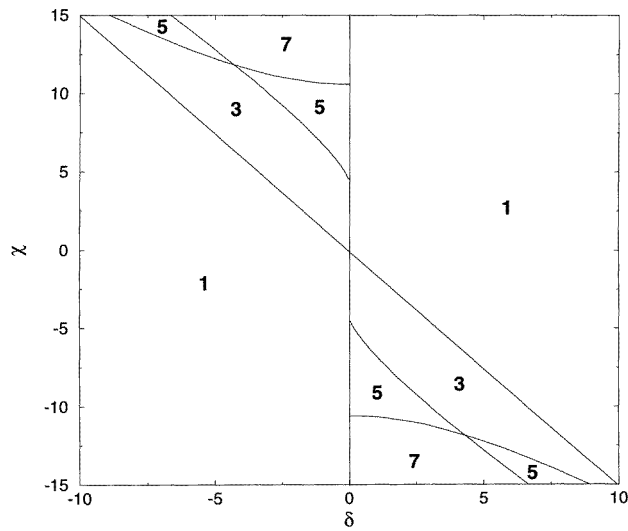


**Figure 6.** The phase diagram of SL states in the  $(\chi, \delta)$  plane for a one-dimensional system with a bond defect between sites 0 and 1 as well as a nondegenerate quadratic nonlinear dimeric impurity occupying sites 0 and 1. The bond defect,  $V$ , is taken to be 2. The number labelling a region indicates the number of SL states possible in that region.

In passing, it is worth mentioning that there are  $N/2$  stable SL states in a region if the region in the phase plane contains  $N$  SL states and  $N$  is even. On the other hand,  $(N + 1)/2$  states are stable if  $N$  is odd. The stability of a SL state is connected to the variation of the energy of the state as a function of  $\chi$ . If the energy of the state increases with the increase



of  $\chi$ , the state is stable; otherwise it is unstable. A simpler analysis of the stability of a state and its connection to the state's energy will be presented in the next section.

### 3. A fully nonlinear chain with alternative nonlinear strengths

Here we consider a fully nonlinear one-dimensional system where the alternative sites are of similar strengths. The Hamiltonian of the system is given by

$$H = \frac{2}{\sigma + 2} \sum_{n=-\infty}^{\infty} \chi_n |C_n|^{\sigma+2} + \sum_{n=-\infty}^{\infty} [C_n^* C_{n+1} + \text{HC}] \quad (13)$$

where

$$\begin{aligned} \chi_{2n} &= \chi_1 & -\infty \leq n \leq \infty \\ \chi_{2n+1} &= \chi_2 & -\infty \leq n \leq \infty. \end{aligned} \quad (14)$$

The hopping matrix elements connecting neighbouring sites are taken to be unity. To obtain the SL states we consider  $C_n = \phi_n e^{-iEt}$  and  $\phi_n = \phi_0 \eta^{|n|}$ . The expression for  $\eta$  is obtained by taking  $|n| \rightarrow \infty$  and is given by

$$\eta = \frac{1}{2} [ |E| - \sqrt{E^2 - 4} ]$$

[21]. Here we have considered a monomeric *ansatz* because the system is symmetric about the 0th site. After going through the same procedure as earlier and using the normalization condition  $|\phi_0|^2 = (1 - \eta^2)/(1 + \eta^2)$ , we obtain the reduced Hamiltonian of the dynamical system:

$$H_{eff} = \frac{2}{(\sigma + 2)} \left[ \frac{1 - \eta^2}{1 + \eta^2} \right]^{(\sigma+2)/2} \left[ \chi \frac{1 + \eta^{\sigma+2}}{1 - \eta^{\sigma+2}} + \delta \frac{1 - \eta^{\sigma+2}}{1 + \eta^{\sigma+2}} \right] + \frac{4\eta}{1 + \eta^2} \quad (15)$$

where  $\chi$  and  $\delta$  are defined as  $\chi = (\chi_1 + \chi_2)/2$  and  $\delta = (\chi_1 - \chi_2)/2$ . Setting  $\partial H_{eff}/\partial \eta = 0$  we get

$$\frac{1}{\chi} = (\eta^\sigma - 1)(\eta^{\sigma+4} + 1) / \left( \left[ \frac{\eta^2 - 1}{\eta} \left( \frac{1 + \eta^2}{1 - \eta^2} \right)^{\sigma/2} - \delta \frac{(\eta^\sigma + 1)(\eta^{\sigma+4} - 1)}{(1 + \eta^{\sigma+2})^2} \right] (1 - \eta^{\sigma+2})^2 \right). \quad (16)$$

Equation (16) can be used to analyse the number of possible states for different values of  $\chi$ ,  $\delta$  and  $\sigma$ . For  $\sigma = 0$  and  $\delta = 0$ , from equation (16) we see that, to get a SL state,  $\chi$  needs to be infinite. This, therefore, means that no SL states can be obtained. This is true for  $\sigma = 0$  and  $\delta = 0$  because for these values the system reduces to a perfect linear system. This is also true for  $\sigma = 0$  and  $\delta \neq 0$ . Analysis of SL states can be performed for arbitrary  $\sigma$  but we consider the case of  $\sigma = 2$  for the reason mentioned earlier. For  $\sigma = 2$ , equation (16) reduces to

$$\frac{1}{\chi} = \frac{\eta(1 + \eta^6)(1 + \eta^4)^2}{(1 + \eta^2)^3 [(1 - \eta^2)(1 + \eta^4)^2 - \delta \eta(1 - \eta^2)(1 - \eta^6)]}. \quad (17)$$

Equation (17) tells us directly that for  $\delta = 0$  there will always be one SL state and this is consistent with our earlier result [24]. Using equation (17), the phase diagram of SL states in the  $(\chi, \delta)$  plane is obtained; this is shown in figure 7. As before, the numbers labelling the different regions indicate the numbers of SL states in those regions. Here also the maximum number of SL states increases compared to that for a perfect nonlinear chain. Furthermore, the phase diagram in this case is quite rich (see figure 7). Stationary localized

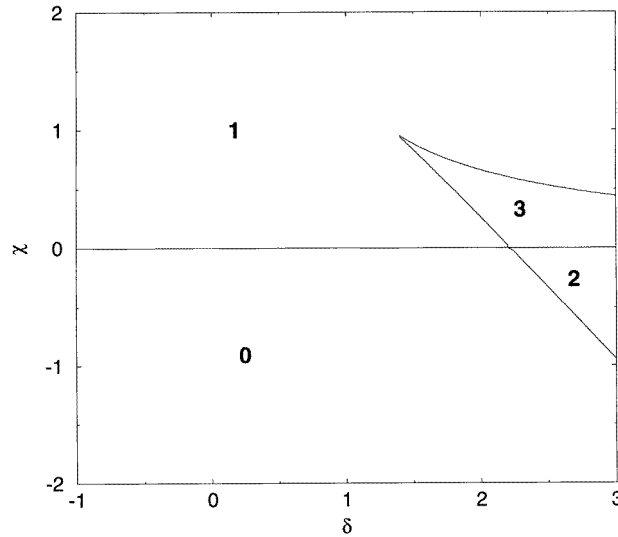


**Figure 7.** The phase diagram of the SL states in the  $(\chi, \delta)$  plane for a fully nonlinear one-dimensional system where alternative sites are of different nonlinear strengths. The number labelling a region indicates the number of SL states possible in that region.

states in linear impure systems are well known to occur [25]. On the other hand, here we have a translationally invariant system. This then shows that nonlinearity can introduce self-localization [26] in the system. This is an interesting result.

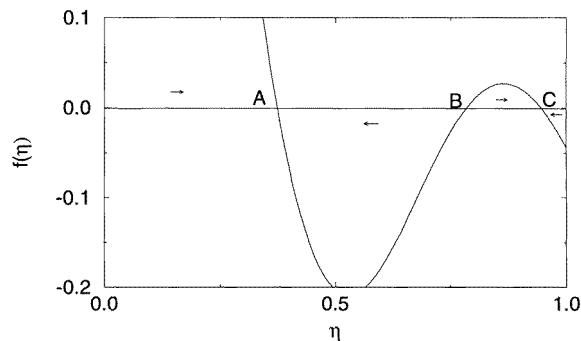


**Figure 8.**  $f(\eta)$  is plotted as a function of  $\eta$ . The points indicated by A, B and C are fixed points. Here  $\chi$  and  $\delta$  are taken to be 0.35 and 2.5 respectively.

The stability of the SL states in this system can be understood from a simpler graphical analysis. For this purpose we look at the Hamiltonian given in equation (15). The Hamiltonian is function of one dynamical variable, namely  $\eta$ , where  $\chi$  and  $\delta$  are parameters. Here we consider an analogous equation,  $\dot{\eta} = \partial H_{eff} / \partial \eta = f(\eta)$ . The solutions of the equation  $f(\eta) = 0$  will give the fixed points for fixed values of  $\chi$  and  $\delta$  and the number of fixed points with  $\eta \in [0, 1]$  will be the number of SL states. We now plot  $f(\eta)$  as a function of  $\eta$  for  $\chi = 0.35$  and  $\delta = 2.5$ ; this is shown in figure 8. If  $f(\eta) > 0$ , then the flow of the dynamical variable will be in the positive direction and, on the other hand, if  $f(\eta) < 0$ , then

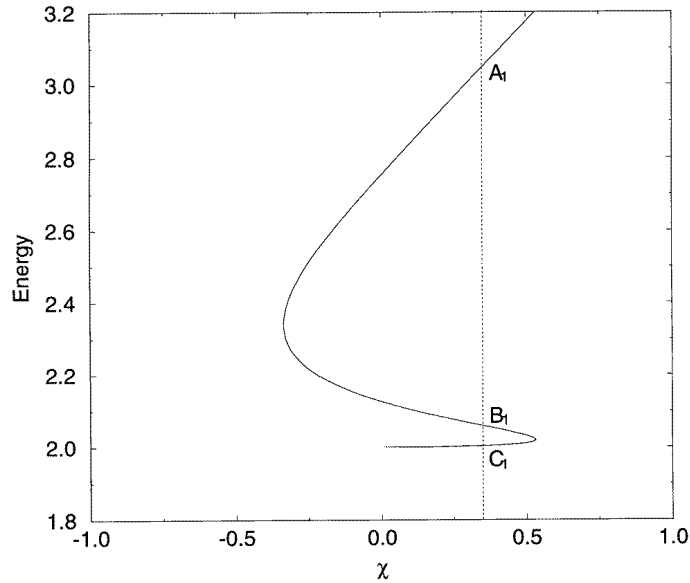


**Figure 9.** The energies of the SL states are plotted as a function of  $\chi$ . Here  $\delta = 2.5$ .  $A_1$ ,  $B_1$  and  $C_1$  are the points corresponding to the points A, B and C (in figure 8) respectively. The dotted line is  $\chi = 0.35$ .

the flow will be in the negative direction. These flows are indicated by arrows in the figure and the fixed points are denoted by A, B and C respectively. In the neighbourhood of A the flow is always towards A and the same is true for C. Therefore, A and C are stable fixed points. On the other hand, in the neighbourhood of B the flow is away from B. Hence, this is an unstable fixed point. The same thing happens for all  $(\chi, \delta)$  in the three-state region in figure 7. We therefore note that among the three SL states (fixed points), two are stable and the other one is unstable.

To find the connection of the stability of the states to the energy and  $\chi$ , we plot the energy of the states as a function of  $\chi$  in the neighbourhood of  $\chi = 0.35$  for a fixed value of  $\delta = 2.5$ ; this is shown in figure 9. The energies of the SL states arising from the fixed points A, B and C are denoted by  $A_1$ ,  $B_1$  and  $C_1$  respectively in figure 9. This figure clearly shows that in the neighbourhood of  $\chi = 0.35$ , the energies of the two stable SL states increase with  $\chi$  and that of the unstable state decreases. We, therefore, conclude that the SL state is stable if the energy of the state increases with  $\chi$  and that otherwise it is unstable.

We now end this section with a brief discussion of the exactness of the calculation. The method adopted here is similar to the well known effective-medium theory for the linear system. This is quite clear from the form of  $H_{eff}$  given in equation (15). A single nonlinear impurity,  $\chi_{eff}$ , which is a function of  $\eta$ ,  $\chi$  and  $\delta$ , can give rise to such a Hamiltonian. Again it is well known that for one-dimensional systems, impurity states appearing outside the band are exponentially localized. Low-energy SL states will peak at a lattice point and will fall exponentially on both sides. So, the use of a monomeric *ansatz* is entirely justified (see also reference [21]). Therefore, the basic features obtained here will also be reproduced by rigorous calculations. However, quantitative agreement may not be obtained. More work is therefore necessary.

#### 4. Summary

We have found the possible numbers of SL states due to the presence of a quadratic nondegenerate nonlinear dimeric impurity in one-dimensional systems. Phase diagrams of the SL states in the  $(\chi, \delta)$  plane are presented for all of the systems with nondegenerate dimeric impurities. The maximum number of SL states possible is found to increase due to the introduction of nondegeneracy. The dimeric *ansatz* has been used in this case and this reproduces known results for special cases. A full phase diagram of the self-localized states for a system comprising a one-dimensional chain with alternative sites having same nonlinear strength is presented. A monomeric *ansatz* has been introduced in this case and found to reproduce known results for special cases. Here also, the maximum number of SL states possible is increased compared to that for a perfect nonlinear system. A stability analysis for the SL states in the fully nonlinear system and a connection between the stability and the variation of the energy of the state as a function of the nonlinear parameter are presented.

#### Appendix

The structure of a Cayley tree with connectivity  $K = Z - 1 = 2$  is shown in figure A1.  $Z$  is the coordination number. We select a connection and number its two ends 0 and 1 without any loss of generality. Furthermore, all points in a given generation lie in a shell. Shells are labelled with numbers  $n$  where  $n \in (-\infty, \infty)$  as shown in figure A1. In a perfect Cayley tree, the number of points in the  $n$ th shell is  $K^{n-1}$  if  $n \geq 1$  and  $K^{|n|}$  if  $n \leq 0$ . We further note that for a perfect Cayley tree all points in a given shell have identical neighbourhoods.

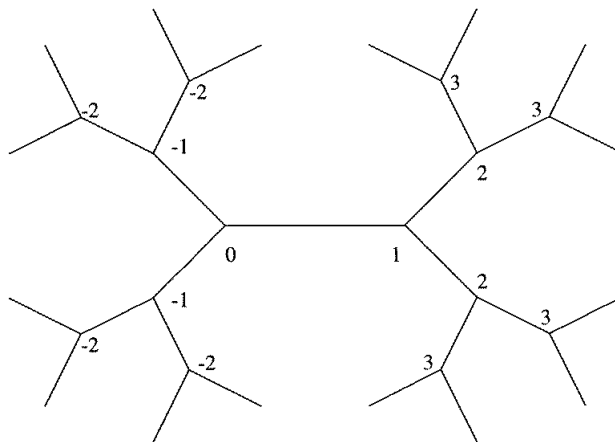


**Figure A1.** This is the Cayley tree with connectivity  $K = 2$ . All of the sites in a given shell are labelled with the same number.

We consider now the motion of a particle on a Cayley tree with connectivity  $K$ . In the tight-binding formalism with nearest-neighbour hopping, the only equations governing the

motion of the particle are

$$\begin{aligned}
 i\frac{d\tilde{C}_n}{dt} &= K\tilde{C}_{n+1} + \tilde{C}_{n-1} + \tilde{\epsilon}_n\tilde{C}_n & n > 1 \\
 i\frac{d\tilde{C}_n}{dt} &= K\tilde{C}_{-|n|-1} + \tilde{C}_{-|n|+1} + \tilde{\epsilon}_n\tilde{C}_n & n < 0 \\
 i\frac{d\tilde{C}_1}{dt} &= K\tilde{C}_2 + \tilde{C}_0 + \tilde{\epsilon}_1\tilde{C}_1 \\
 i\frac{d\tilde{C}_0}{dt} &= K\tilde{C}_{-1} + \tilde{C}_1 + \tilde{\epsilon}_0\tilde{C}_0.
 \end{aligned} \tag{A1}$$

Here  $\tilde{C}_n$  denotes the probability amplitude at any point in the  $n$ th shell, and all points in the  $n$ th cell have the same probability amplitude because of the identical neighbourhoods. The nearest-neighbour hopping matrix has been taken to be the identity matrix without any loss of generality. It is also assumed that all points in a given shell arising due to a specific organization have the same site energy. We note that in our work with the DNLSSE, this assumption is automatically satisfied. The normalization condition for the site amplitudes gives

$$\sum_{n=-\infty}^0 K^{|n|} |\tilde{C}_n|^2 + \frac{1}{K} \sum_{n=1}^{\infty} K^n |\tilde{C}_n|^2 = 1. \tag{A2}$$

We now carry out the following transformations: (i)  $\tau = \sqrt{K}t$ ; (ii)  $\epsilon_n = \tilde{\epsilon}_n/\sqrt{K}$ , (iii)  $\tilde{C}_n = K^{-(n-1)/2}C_n$  for  $n \geq 1$ ; and (iv)  $\tilde{C}_{-|n|} = K^{-|n|/2}C_n$  for  $n \leq 0$ . After substituting these transformations in equation (18), we finally obtain

$$\begin{aligned}
 i\frac{dC_n}{d\tau} &= C_{n+1} + C_{n-1} + \epsilon_n C_n & \text{for } n > 1 \text{ and } n < 0. \\
 i\frac{dC_1}{d\tau} &= C_2 + VC_0 + \epsilon_1 C_1 \\
 i\frac{dC_0}{d\tau} &= C_{-1} + VC_1 + \epsilon_0 C_0
 \end{aligned} \tag{A3}$$

where  $V = 1/\sqrt{K}$ . Furthermore, from equation (19) the normalization condition reduces to  $\sum_{-\infty}^{\infty} |C_n|^2 = 1$ . So, the motion of a particle on a Cayley tree is mapped to that on a one-dimensional chain. However, in this chain the nearest-neighbour hopping matrix element connecting the zeroth and first sites is reduced from unity to  $V = 1/\sqrt{K}$ . Since for the Cayley tree  $K \geq 2$ ,  $V < 1$ .

Since we are interested in the DNLSSE with a general power-law nonlinear impurity, in our case

$$\epsilon_n = \tilde{\epsilon}_n/\sqrt{K} = \tilde{\chi}_n K^{-(n-1)\sigma/2} K^{-1/2} |C_n|^\sigma \quad \text{for } n \geq 1$$

and

$$\epsilon_{-|n|} = \tilde{\epsilon}_{-|n|}/\sqrt{K} = \tilde{\chi}_{-|n|} K^{-|n|\sigma/2} K^{-1/2} |C_{-|n|}|^\sigma \quad \text{for } n \geq 0.$$

Furthermore,  $\chi_n = \tilde{\chi}_n/\sqrt{K}$ . Thus, we see that when  $\chi_n = \chi_0\delta_{n,0} + \chi_1\delta_{n,1}$ ,  $-\infty < n < \infty$ , equation (20) can be generated from the Hamiltonian given by equation (2) with  $V < 1$ . We further note that the Green's function calculated from equation (20) will yield  $\tilde{G}_{0,0}(\tilde{E} = E/V)$  for a perfect Cayley tree with connectivity  $K$  when  $KV^2 = 1$ . Consequently, the general Green's function can be calculated [24].

## References

- [1] Holstein T D 1959 *Ann. Phys., Lpz.* **8** 325  
Holstein T D 1959 *Ann. Phys., Lpz.* **8** 343  
Turkevich L A and Holstein T D 1987 *Phys. Rev. B* **35** 7474
- [2] Eilbeck J C, Lomdahl P S and Scott A C 1985 *Physica D* **16** 318
- [3] Christiansen P L and Scott A C 1991 *Davydov's Soliton Revisited: Self-Trapping of Vibrational Energy in Protein (NATO ASI Series B: Physics, vol 243)* (New York: Plenum)
- [4] Emin D 1982 *Phys. Today* **35** (6) 34
- [5] Toyozawa Y 1983 *Organic Molecular Aggregates* ed P Reineker, H Haken and H C Wolf (Berlin: Springer)
- [6] Campbell D K, Bishop A R and Fesser K 1982 *Phys. Rev. B* **26** 6862
- [7] Chen D, Molina M I and Tsironis G P 1993 *J. Phys.: Condens. Matter* **5** 8689
- [8] Wan Y and Soukoulis C M 1989 *Phys. Rev. B* **40** 12264
- [9] Molina M I and Tsironis G P 1994 *Phys. Rev. Lett.* **73** 464
- [10] Kenkre V M, Tsironis G P and Campbell D K 1987 *Nonlinearity in Condensed Matter* ed A R Bishop, D K Campbell, P Kumar and S E Trullinger (Berlin: Springer)
- [11] Cohen M H, Economou E N and Soukoulis C M 1983 *Phys. Rev. Lett.* **51** 1202
- [12] Chen W and Mills D L 1987 *Phys. Rev. Lett.* **58** 160
- [13] Abrikosov A A, Buzdin A I and Kucic M L 1989 *Supercond. Sci. Technol.* **1** 260
- [14] Claude C, Kivshar Y S, Kluth O and Spatschek K H 1993 *Phys. Rev. B* **47** 14228
- [15] Dauxois T, Peyrard M and Bishop A R 1993 *Phys. Rev. E* **47** 684
- [16] Cai D, Bishop A R and Gronbeck-Jensen N 1994 *Phys. Rev. Lett.* **72** 591
- [17] Tsironis G P, Molina M I and Hennig D 1994 *Phys. Rev. E* **50** 2365  
Molina M I and Tsironis G P 1993 *Phys. Rev. B* **47** 15330
- [18] Yiu Y Y, Ng K M and Hui P M 1995 *Phys. Lett.* **200A** 325  
Yiu Y Y, Ng K M and Hui P M 1995 *Solid State Commun.* **95** 801
- [19] Hui P M, Woo Y F and Deng W 1996 *J. Phys.: Condens. Matter* **8** 2011
- [20] Gupta B C and Kundu K 1997 *Phys. Rev. B* **55** 894
- [21] Malomed B and Weinstein M I 1996 *Phys. Lett.* **220A** 91
- [22] Aceves A B, De Angelis C, Peschel T, Muschall R, Lederer F, Trillo S and Wabnitz S 1996 *Phys. Rev. E* **53** 1172
- [23] Gupta B C and Kundu K 1997 *Phys. Rev. B* **55** 11033
- [24] Gupta B C and Kundu K 1997 *Phys. Lett.* **235A** 176  
Kundu K and Gupta B C 1998 *Eur. Phys. J. B* at press
- [25] Economou E N 1983 *Green's Functions in Quantum Physics* (Berlin: Springer)
- [26] Bonart D, Mayer A and Schroeder 1995 *Phys. Rev. Lett.* **75** 870